Available online at www.CivileJournal.org

Civil Engineering Journal

Vol. 3, No. 10, October, 2017

Construction of N-M Interaction Diagram for Reinforced Concrete Columns Strengthened with Steel Jackets Using Plastic Stress Distribution Method

Mohannad H. Al-Sherrawi [a*], Hamza M. Salman [a]

[a] *University of Baghdad, Department of Civil Engineering, 10071, Baghdad, Iraq.*

Received 4 September 2017; Accepted 25 October 2017

Abstract

No attempts have been made in developing the N-M interaction diagram for reinforced concrete columns strengthened with steel jackets using the plastic stress distribution method. Therefore, this paper presents an analytical model to construct the N-M interaction diagram for reinforced concrete columns strengthened with steel jackets using the plastic stress distribution method after assuming the behavior of strengthened column to be like composite column and including the effects of confinement on concrete compressive strength. The proposed model was compared with experimental results. The comparisons showed that the model is conservative and it reveals the ultimate strength of the strengthened column. A parametric study has been also carried out to investigate the influence of various parameters on the N-M interaction diagram of the strengthened column. These parameters were: dimensions of steel angle, yield stress of the steel angles, concrete compressive strength and the size of the reinforcement bars used in RC columns. The results made clear the effects of these parameters on the N-M interaction diagram, and encouraged the use of the model in preliminary strengthening studies.

Keywords: Interaction Diagram; Reinforced Concrete Columns; Steel Jacket; Plastic Stress Distribution; Composite Column.

1. Introduction

There are a number of design proposals that can be used to construct N-M interaction diagram for a composite steel-reinforced concrete column which are: the Wakabayashi's method, the American Structural Specifications Liaison Committee method, the Roik-Bergmann method, the Eurocode No.4 method and others [1]. All these methods did not construct the N-M interaction diagram for reinforced concrete column strengthened with steel jacket.

This paper presents an analytical model for the construction of interaction diagram for RC column strengthened with steel angles and strips using the plastic stress distribution method. In this work and due to placing of steel cage, the effects of confinement on concrete compressive strength, stress-strain response of confined concrete will be taken into consideration by assuming the column is acting like concrete filled tube section. The angles were assumed to be bonded to the concrete by filling the gaps between the concrete and steel jacket with injection plaster or a concrete mortar forming a layer of binding material between the concrete and steel jacket. At first, the proposed model is verified with experimental results, and then a parametric study is carried out to investigate the influence of some parameters.

* Corresponding author: Dr.Mohannad.Al-Sherrawi@coeng.uobaghdad.edu.iq

http://dx.doi.org/10.28991/cej-030926

2. Literature Review

Garzón et al. 2012 [2] presented a finite element model of a RC column strengthened with steel caging subjected to bending moments and axial loads. The model is used to obtain the N-M diagrams, studying the difference between fitting and not capitals at the end of the strengthened RC column, next to the beam-column joint. In addition the model is used to perform a parametric study in which it is investigated the influence of several parameters.

Equations for a hand computation of moment-axial forced domain of RC columns externally strengthened with steel angles and strips are developed by Campione 2013 [3]. The analytical derivation was made assuming equivalent stress-block parameters for internal force considering the confinement effect induced in concrete core by external cages. The proposed model gave results in a good agreement with experimental data.

Christou et al. 2013 [4] evaluated experimentally the effect of three levels of confinement with the use of a CFRP composite grid on the interaction diagram of RC columns. The comparison showed a considerable difference primarily in the compression-controlled region where the axial compression and bending moment are significantly enhanced.

Patel and Panchal 2016 [5] presented a simplified method for development of N-M interaction chart for concrete filled tube composite columns. The method was based on simple European buckling curves for composite columns.

Al-Sherrawi and Salman 2017 [6] presented two analytical models to construct the axial load-bending moment interaction diagram of a RC column strengthened with steel jacket. The derivation of expressions was made by assuming equivalent stress block parameters for confined concrete. The proposed models show good agreements with available experimental data and design proposals.

3. Methodology

The four points identified in Figure 1. are defined by the plastic stress distribution used in their determination. Point A is the pure axial strength, Point B is determined as the flexural strength of the section, Point D corresponds to maximum flexural strength with an axial strength, and Point C corresponds to a plastic neutral axis location that results in the same flexural capacity as Point B but with twice the axial load of Point D. The main dimensions of the strengthened concrete column used are given in Figure 2. For any position of neutral axis (c), stresses of reinforcing bars and steel angles will be f_{yr} and f_{ya} respectively, while the stress block of concrete will be f_c as width due to effects of confinement and αc as height, and α was assumed to be 0.85. The description of each one of the four points is expressed below:

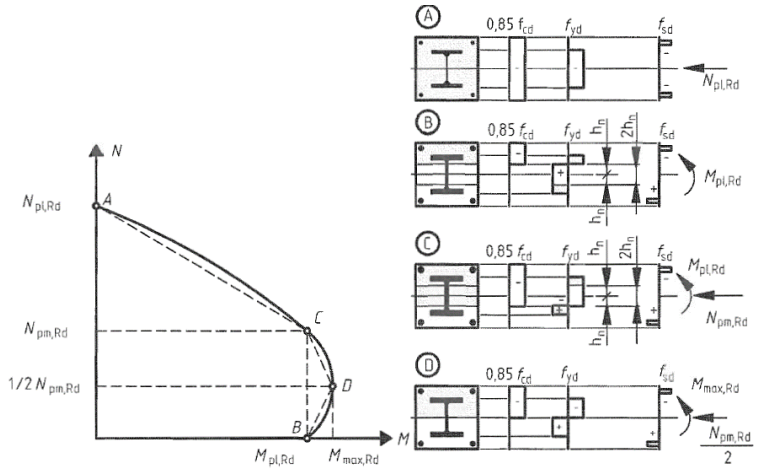

Figure 1. The interaction diagram for composite column [7]

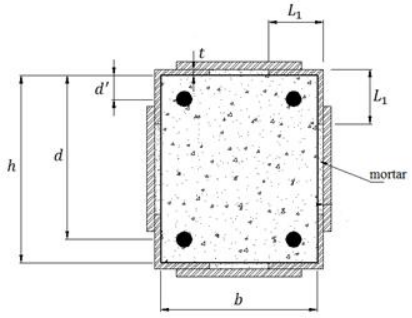

Figure 2. Details and dimensions of RC column and steel cage

Point A is defined with the design value of the resistance of the composite section to compressive axial force N_A while the bending moment M_A is zero (eccentricity $e = 0$) (Figure 3).

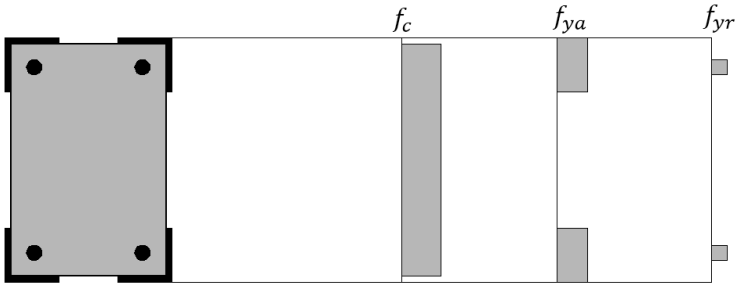

Figure 3. Stress distribution for point A

$$\begin{aligned} N_A &= f_c bh + f_{ya}A_s + f_{yr}A_{sr} \\ M_A &= 0 \end{aligned} \quad (1)$$

Where b is the width of column, h is the height of column, A_s is the total area of steel angles, and A_{sr} is the total area for reinforcing bars.

Point D is defined with the maximum design value of the resistance moment M_D in the presence of a compressive normal force N_D (Figure 4).

$$N_D = f_c \frac{h}{2} b \quad (2)$$

$$M_D = M_{max} = f_c \left[\frac{bh^2}{8}\right] + Z_a f_{ya} + f_{yr}A_{sr}\left[d - \frac{h}{2}\right] \quad (3)$$

Where αc is the height of equivalent stress block, d is the effective depth for reinforcing bars, and Z_a is the plastic section modulus for steel angles.

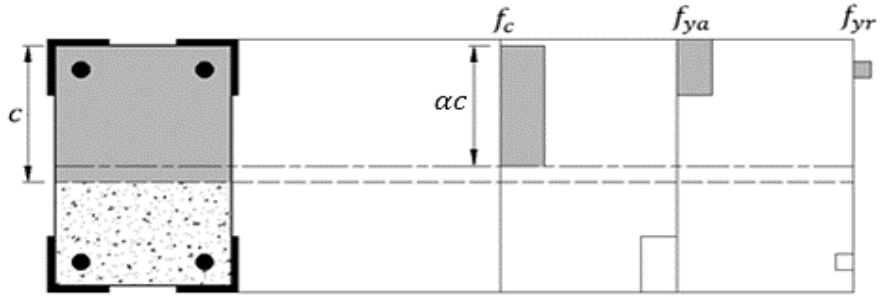

Figure 4. Stress distribution for point D

$$Z_a = 4\left[\left[(L_1 - t)t\left(\frac{h+t}{2}\right)\right] + \left[L_1 t\left(\frac{h}{2} + t - \frac{L_1}{2}\right)\right]\right] \quad (4)$$

Point B is defined with the design value of the bending moment resistance the composite section M_B while the axial force N_B is zero (eccentricity $e = \infty$). The position of neutral$c$ axis must be assumed and to be checked later. By applying $\sum F = N_B$ and using $N_B = 0$, c can be found. In this paper four possible assumptions may be considered to find c and as follows:

Case 1: $(L_1 - t) \leq c < \frac{h}{2}$ as shown in Figure 5.

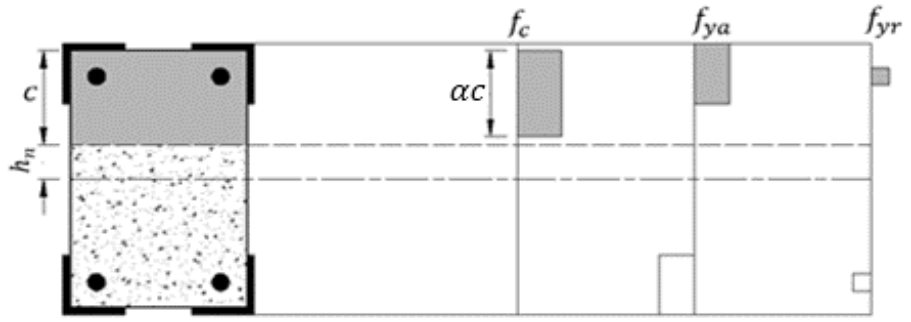

Figure 5. Stress distribution for case 1

$N_B = 0$

$$f_c\, b\alpha c + \frac{A_s}{2} f_{ya} + \frac{A_{sr}}{2} f_{yr} - \frac{A_s}{2} f_{ys} - \frac{A_{sr}}{2} f_{yr} = 0$$

$$f_c\, b\alpha c = 0$$

$f_c\, b\alpha \neq 0$
$c = 0$ (Error)

Case 2: $0 < c < (L_1 - t)$ *and* $c \geq \left(d' + \frac{d_{bar}}{2}\right)$ as shown in Figure 6.

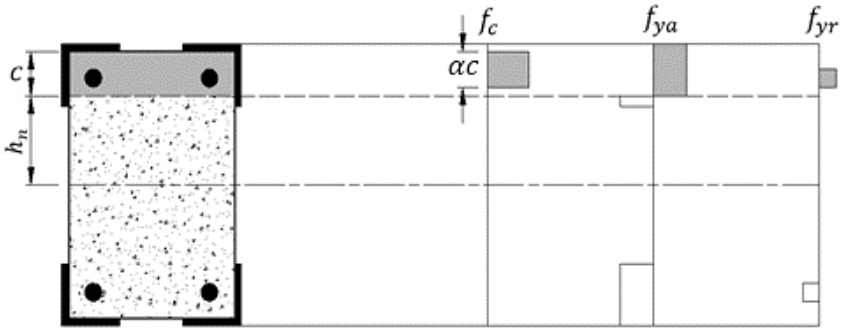

Figure 6. Stress distribution for case 2

$N_B = 0$

$$f_c\, b\alpha c + \frac{A_s}{2} f_{ya} + \frac{A_{sr}}{2} f_{yr} - \frac{A_s}{2} f_{ya} - \frac{A_{sr}}{2} f_{yr} - 4\left(t f_{ya}(L_1 - t - c)\right) = 0$$

$$c = \frac{4 t f_{ya}(L_1 - t)}{\alpha\, f_c\, b + 4 t f_{ya}} \tag{5}$$

$$h_n = \frac{h}{2} - c$$

$$M_B = f_c\, b\alpha c\left(\frac{h}{2} - \frac{\alpha c}{2}\right) + Z_a\, f_{ya} + A_{sr}\, f_{yr}\left(\frac{h}{2} - d'\right) - \left[4t(L_1 - t - c) f_{ya}\left(\frac{h}{2} - c - \left(\frac{L_1 - t - c}{2}\right)\right)\right] \tag{6}$$

Case 3: $0 < c < (L_1 - t)$ *and* $\left(d' - \frac{d_{bar}}{2}\right) < c < \left(d' + \frac{d_{bar}}{2}\right)$ as shown in Figure 7.

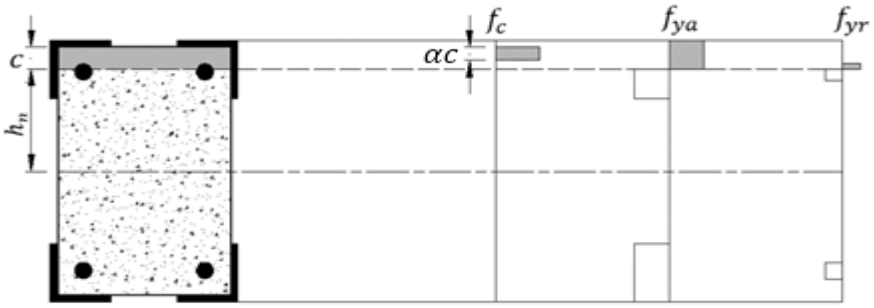

Figure 7. Stress distribution for case 3

$A_i = d_{bar} h_i$

$h_i = c - concrete\ cover - d_{tie}$

Where A_i is the area of the segment of reinforcing bars under compressive stress and h_i is the height of this segment. The center of gravity of this segment can be assumed as $\frac{h_i}{2}$.

$$N_B = 0$$

$$f_c\, b\alpha c + \frac{A_s}{2} f_{ya} + \frac{n}{2} A_i f_{yr} - \left(\frac{A_{sr}}{2} - \frac{n}{2} A_i\right) f_{yr} - \frac{A_{sr}}{2} f_{yr} - \frac{A_s}{2} f_{ya} - 4\big(t(L_1 - t - c) f_{ya}\big) = 0$$

Where n is the number of reinforcing bars.

$$c = \frac{4t(L_1 - t) f_{ya} + (A_{sr} - nA_i) f_{yr}}{f_c\, \alpha b + 4\, t f_{ya}} \tag{7}$$

$$h_n = \frac{h}{2} - c$$

$$M_B = f_c\, b\alpha c\left(\frac{h}{2} - \frac{\alpha c}{2}\right) + Z_s\, f_{ya} - \left[4t(L_1 - t - c) f_{ya}\left(\frac{h}{2} - c - \left(\frac{L_1 - t - c}{2}\right)\right)\right] + \frac{n}{2} A_i f_{yr}\left(\frac{h}{2} - c + \frac{h_i}{2}\right) - \left[\left(\frac{A_{sr}}{2} - \frac{n}{2} A_i\right) f_{yr}\left(\frac{h}{2} - c - \left(\frac{d_{bar} - h_i}{2}\right)\right)\right] + \frac{A_{sr}}{2}\, f_{yr}\left(\frac{h}{2} - d'\right) \tag{8}$$

Case 4: $0 < c < (L_1 - t)$ *and* $c \le \left(d' - \frac{d_{bar}}{2}\right)$ as shown in Figure 8.

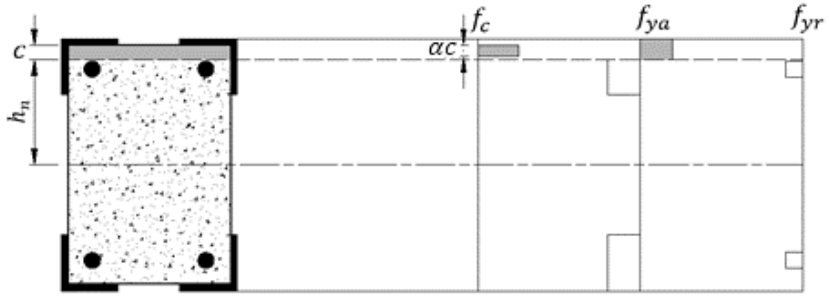

Figure 8. Stress distribution for case 4.

$$N_B = 0$$

$$f_c\, b\alpha c + \frac{A_s}{2} f_{ya} - A_{sr} f_{yr} - \frac{A_s}{2} f_{ya} - 4\big(t(L_1 - t - c) f_{ya}\big) = 0$$

$$c = \frac{4t(L_1 - t) f_{ya} + A_{sr} f_{yr}}{f_c \alpha b + 4 f_{ya}\, t} \tag{9}$$

$$h_n = \frac{h}{2} - c$$

$$M_B = f_c\, b\alpha c\left(\frac{h}{2} - \frac{\alpha c}{2}\right) + Z_s\, f_{ys} - \left[4t(L_1 - t - c)f_{ya}\left(\frac{h}{2} - c - \left(\frac{L_1 - t - c}{2}\right)\right)\right] \quad (10)$$

Point C corresponds to a neutral axis location that results in the same flexural capacity as Point B and twice the axial load of Point D.

$$N_C = 2N_D$$

$$M_C = M_B$$

4. Validation of Analytical Model

A set of an experimental investigations presented by Garzon et al. [8] (A-800-a, A-1200-b) and Ezz-Eldeen [9] (CS22e1, CS22e2, CS22e3 and CS22e4) were used to validate the presented model. The Details of these models are illustrated in Table 1. For each set, an N-M interaction diagram has been drawn (Figures 9 and 10).

Table 1. Details of selected columns and obtained results.

Model	Cross-section (mm)	Steel angle (mm)	Longitudinal bars	f'_c (MPa)	f_{ya} (MPa)	f_{yr} (MPa)	e (mm)	Experimental results		Analytical results		Comparison	
								$N_{exp.}$	$M_{exp.}$	$N_{ana.}$	$M_{ana.}$	$\frac{N_{ana}}{N_{exp}}$	$\frac{M_{ana}}{M_{exp}}$
A-800-a	260 × 260	4 L 60 × 6	4 φ 12 mm	12	275	500	----	800	99.7	900	105	1.12	1.05
A-1200-b	260 × 260	4 L 60 × 6	4 φ 12 mm	12	275	500	----	1200	72.6	1190	72	0.99	0.99
CS22e1	120 × 160	4 L 20 × 2	4 φ 8 mm	25	380	260	10	643	6.4	603	6.0	0.94	0.94
CS22e2	120 × 160	4 L 20 × 2	4 φ 8 mm	25	380	260	20	552	11.0	519	10.4	0.94	0.94
CS22e3	120 × 160	4 L 20 × 2	4 φ 8 mm	25	380	260	30	474	14.2	457	13.7	0.96	0.96
CS22e4	120 × 160	4 L 20 × 2	4 φ 8 mm	25	380	260	40	420	16.8	407	16.3	0.97	0.97

5. Comparison with Experimental Results

Figures 9 and 10. show the compression of the experimental results with N-M interaction diagram for the analytical model. However, the results are presented in Table 1. Comparisons show that the interaction diagrams obtained by the analytical model give good values comparative with experimental results.

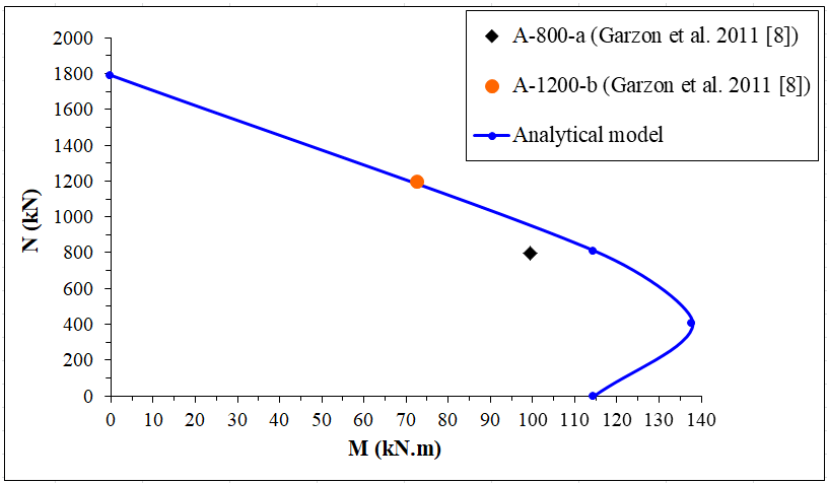

Figure 9. Comparison of experimental results of Garzon et al. [8] with N–M interaction diagram for the analytical model

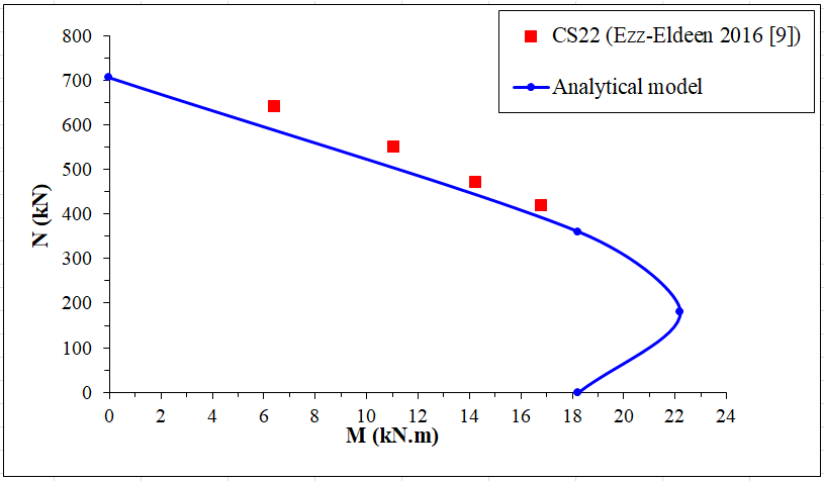

Figure 10. Comparison of experimental results of Ezz-Eldeen [9] with N–M interaction diagram for the analytical model

As it can be seen, the analytical model gives nearby values compared to experimental results. The proposed model is almost conservative, which is preferable in design works.

6. Parametric Study

A parametric study based on the column presented by Garzon et al. [8] was carried out to investigate the influence of various parameters on the interaction diagram of the strengthened column. Some of these parameters related to the steel cage and others related to the RC column itself. These parameters were: dimensions of steel angle, yield stress of the steel angles, concrete compressive strength and the size of the reinforcement bars used in RC columns. Table 2 summarizes the characteristics of the specimens analyzed in this parametric study. The results of parametric study are discussed below.

Table 2. The characteristics of the specimens analyzed in the parametric study

Specimen	Cross-section (mm)	Steel angle (mm)	Longitudinal bars	f'_c (MPa)	f_{ya} (MPa)	f_{yr} (MPa)
1	260 × 260	4 L 60 × 6	4 φ 12 mm	12	275	500
2	260 × 260	4 L 50 × 5	4 φ 12 mm	12	275	500
3	260 × 260	4 L 70 × 7	4 φ 12 mm	12	275	500
4	260 × 260	4 L 80 × 8	4 φ 12 mm	12	275	500
5	260 × 260	4 L 60 × 6	4 φ 12 mm	12	355	500
6	260 × 260	4 L 60 × 6	4 φ 12 mm	20	275	500
7	260 × 260	4 L 60 × 6	4 φ 12 mm	30	275	500
8	260 × 260	4 L 60 × 6	4 φ 10 mm	12	275	500
9	260 × 260	4 L 60 × 6	4 φ 16 mm	12	275	500
10	260 × 260	4 L 60 × 6	4 φ 20 mm	12	275	500

6.1. Dimensions of Steel Angle

Figure 11. shows the effect of changing the dimensions of the steel angles on N-M interaction diagram. Using a larger size of the steel angles increases the axial resistance of a strengthened RC column. Also, Using a larger size of the steel angles gives higher flexural resistance due to increasing of Z_a. The axial resistance in points D and C did not change because the axial resistance in these points depend on the concrete compressive strength only.

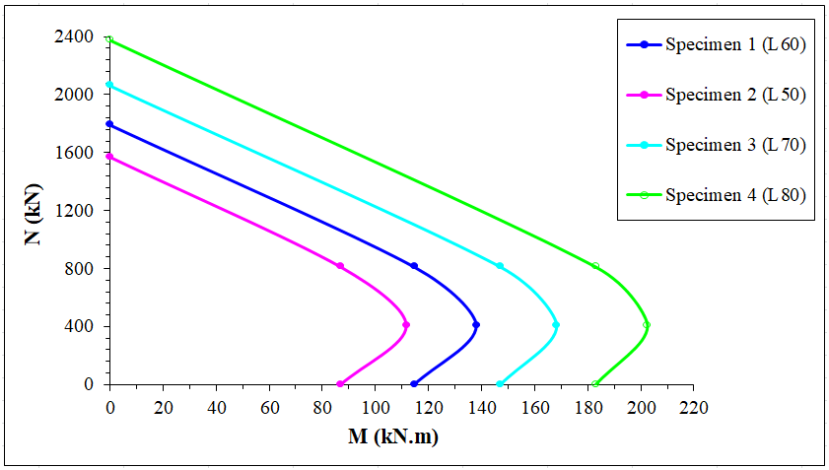

Figure 11. Parametric study; steel angle dimensions

It is interesting to note that the effectiveness of the strengthening highly depends on the dimensions of the steel angles. An increase in it provides a significant improvement in the maximum bending moment.

6.2. Yield Stress of the Steel Angles

As can be seen in Figure 12, the increasing in the yield stress of steel angles will increase the axial resistance of a strengthened RC column; also the larger value of the yield stress gives higher flexural resistance. The axial resistance in point D and C did not change because the axial resistance in these points depends on the concrete compressive strength only.

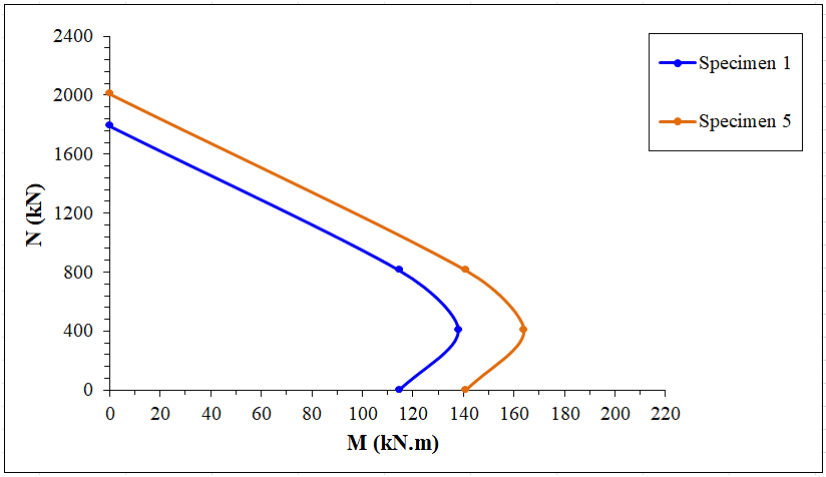

Figure 12. Parametric study; yield stress of steel angles

6.3. Concrete Compressive Strength

The concrete compressive strength (f_c) in the column has no considerable influence on the bending resistance of the strengthened RC column unlike the axial resistance, as shown in Figure 13.

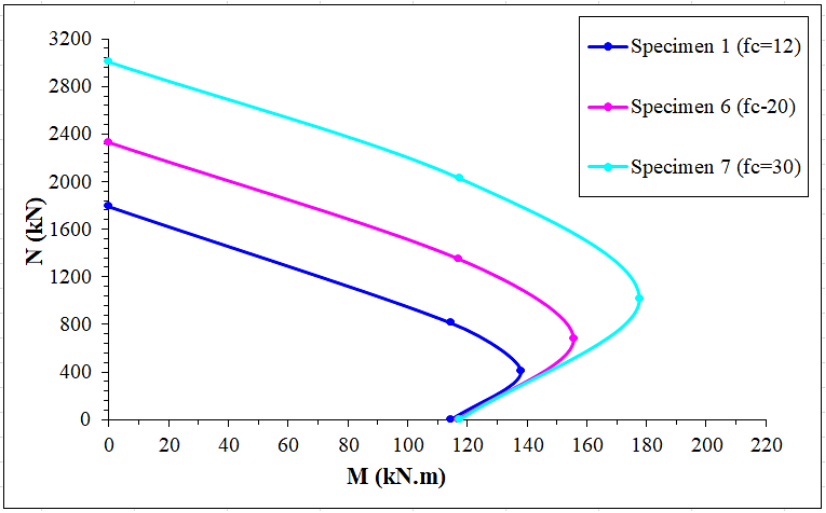

Figure 13. Parametric study; Concrete compressive strength.

6.4. Size of Reinforcement Bars

As can be seen in Figure 14, an increase in reinforcement bars size will increase both of the axial and the flexural resistance. The axial resistance in point C and D did not change because the axial resistance in these points depends on the concrete compressive strength only.

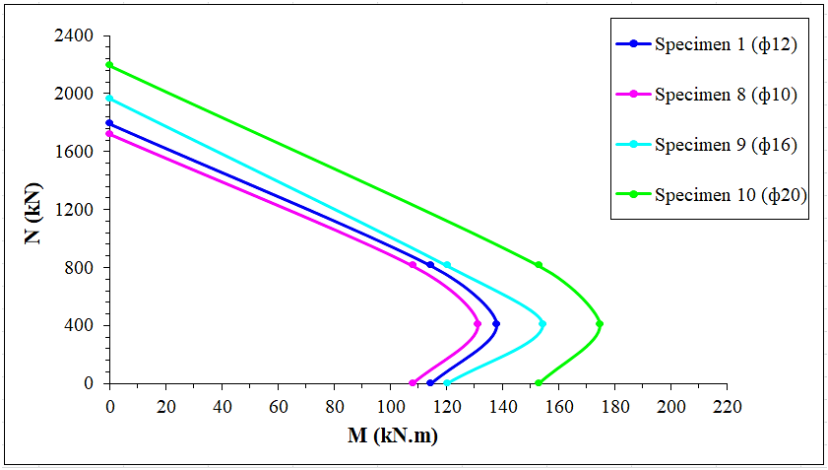

Figure 14. Parametric study; Size of reinforcement bars

7. Conclusion

In the present work an analytical model is derived for the hand computation to construct the N-M interaction diagram for a RC column strengthened with steel jacket using the plastic stress distribution method by assuming the strengthened column behaving as a composite column. The results obtained by the proposed analytical model showed fairly good agreement with the experimental results. Comparisons showed that the analytical model gives almost lower values than experimental results. A parametric study also has been adopted in this work to investigate the effect of four factors.

Results obtained from the parametric study show a clear increase in the ultimate strength of a RC column strengthened with steel jacket with increase in dimensions of steel angles, yield stress of the steel angles, concrete compressive strength and the size of the reinforcement bars. The model is an encouraging trend which may be useful for many practical applications.

8. References

[1] Valach P, and Gramblicka S, "Theoretical and experimental analyses of composite steel-reinforced concrete (SRC) columns." Slovak Journal of Civil Engineering (2007): 1-9.

[2] Garzón-Roca, Julio, Jose M. Adam, Pedro A. Calderón, and Isabel B. Valente. "Finite element modelling of steel-caged RC columns subjected to axial force and bending moment." Engineering Structures 40 (2012): 168-186.

[3] Campione G, “Simplified analytical model for R.C. columns externally strengthened with steel cages.” Journal of Civil

Engineering and Science, 2(4) Dec. (2013): 212-282.

[4] Christou P, Michael A, Anastasiou C, and Nicolaides D, "Effect of confinement on the interaction diagrams for RC sections with CFRP Grids and wraps." Int. J. Comp. Meth. and Exp. Meas. 1(3) (2013): 265–282.

[5] Patel H C, and Panchal D R, "Development of P-M interaction chart for concrete filled tube (CFT) composite columns." International Journal of Advanced Research in Science and Engineering 5(4) (2016): 122-130.

[6] Al-Sherrawi M H and Salman H M, "Analytical model for construction of interaction diagram for RC columns strengthened by steel jacket." International Journal of Science and Research, 6(10) Oct. (2017): 324-328.

[7] CEN 1994-1-1 Eurocode 4, Design of composite steel and concrete structures. Part 1: general rules and rules for buildings, Brussels (Belgium) (2004).

[8] Garzon R J, Adam J M, Pinilla J R, and Calderon P A, "An experimental study on steel-caged RC columns subjected to axial force and bending moment." Engineering Structures, 33 (2011): 580–590.

[9] Ezz-Eldeen H. A. "Steel jacketing technique used in strengthening reinforced concrete rectangular columns under eccentricity for practical design applications" International Journal of Engineering Trends and Technology, 35(5) May (2016): 195-204.